

Scaling Effective Diameters of Small Impact Crater Clusters on Mars J.-P.

Williams¹ and A. V. Pathare², ¹Earth and Space Sciences, University of California, Los Angeles, CA, 90095, USA (jpierre@mars.ucla.edu), ²Planetary Science Institute, Tucson, AZ, USA

Introduction: The High Resolution Imaging Science Experiment (HiRISE) has imaged and confirmed >200 small (<50 m diameter) fresh impact craters having formed within the last 10 years (e.g. [1][2][3][4][5]). This offers an opportunity to study the smallest, meter-scale, craters on the surface of Mars in greater detail. These craters provide a means for dating very young surfaces and isolating smaller regions of interest as these craters form on annual time scales. Approximately half of the fresh craters on Mars are observed to be crater clusters resulting from disruption of the projectile prior to impacting the surface. Large meteor-fireballs are observed to commonly fragment in the terrestrial atmosphere [6]. In order to include cluster forming impact events in the size-frequency distribution (SFD) for comparison with the modeled isochrons, the individual craters of the cluster can be “reconstituted” into a single effective crater created by an equivalent non-fragmented projectile with a diameter $D_{eff} = (\sum D_i^3)^{1/3}$ [1][3]. This provides a simple, effective way to account for the differences in deceleration and ablation experienced by the larger projectile or projectile size dependence on crater scaling. Here we examine how crater scaling and the atmosphere can influence D_{eff} .

Atmospheric entry: Deceleration is proportional to $v_p^2 A/m_p$, or v_p^2/D_p where v_p , A , m_p , and D_p are projectile velocity, cross-sectional area, mass, and diameter respectively. Smaller objects, while having smaller A , also have smaller mass and can be stopped by the atmosphere more effectively. Deceleration becomes significant when $m_p \sim \rho_o H A$ where ρ_o is atmosphere surface density and H is the atmosphere density scale height (i.e. mass of projectile is equivalent to the mass of the atmospheric column beneath) [7]. Assuming an exponential atmosphere density profile, $\rho_a = \rho_o \exp(-z/H)$, the ratio of the final to initial mass of a meteoroid is $\exp[\sigma(v_f^2 - v_i^2)]$ [8], and the smaller objects, experiencing greater deceleration, will also experience greater ablation. If the dynamic pressure, $\rho_a v^2$, exceeds the bulk strength of the meteoroid during flight, fragmentation occurs. The bulk strength inferred from the observed fragmentation altitudes in the terrestrial atmosphere is variable ($\sim 0.1 - 10$'s MPa) [6][9]. Fig 1 shows the fragmentation altitude for a range of entry velocities (5 - 15 km s⁻¹),

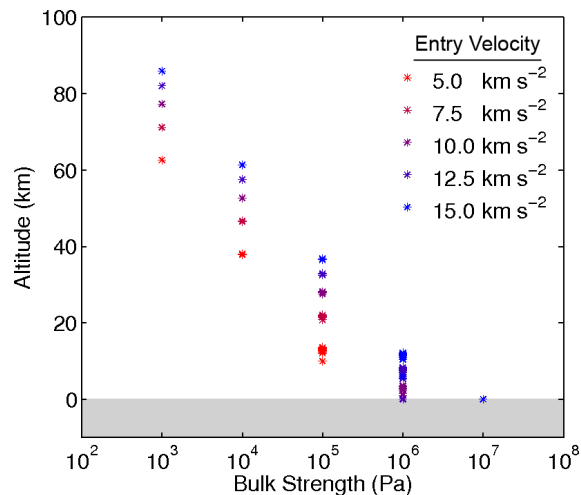


Figure 1: Fragmentation altitude, z_f , versus bulk meteoroid strength in the martian atmosphere. Color indicates initial projectile velocity. Diameter and entry angle only influence z_f for projectiles penetrating deep into the atmosphere.

initial meteoroid diameters (0.5 - 10 m), and entry angles (15° - 90°). As expected, velocity is the predominant factor in fragmentation altitude for a given bulk strength with angle and diameter having a smaller influence within ~ 10 km of the surface where ablation and deceleration become more significant. Given typical bulk strengths, fragmentation can be expected to occur at altitudes <40 km.

Crater scaling: Resulting crater sizes are determined using pi-group scaling assuming parameters of dry soil with effective strength, $\bar{Y} = 65$ kPa [10]. The cratering efficiency, $\pi_v = \rho_t V/m_p$, where ρ_t is the target density and V is the transient crater volume, is proportional to $(\pi_2 + \pi_3 \frac{2+\mu}{2})^{-\frac{3\mu}{2+\mu}}$, assuming impactor and target densities are the same, where μ is an empirical constant (ranging from $\frac{1}{3} - \frac{2}{3}$), $\pi_2 \sim g D_p/v_p^2$ is the gravity-scaled size and $\pi_3 \sim \bar{Y}/\rho_t v_p^2$ is the non-dimensional strength. For very small projectiles, the π_2 term is negligible and π_v becomes constant with impactor size, depending only on velocity and the material strength of the target. At large impactor sizes, π_2 dominates and the cratering efficiency is then dependent not only on velocity, but impactor size.

Results: We model the descent of meteoroid fragments of different masses, velocities, and source altitudes and compare the resulting D_{eff} as a func-

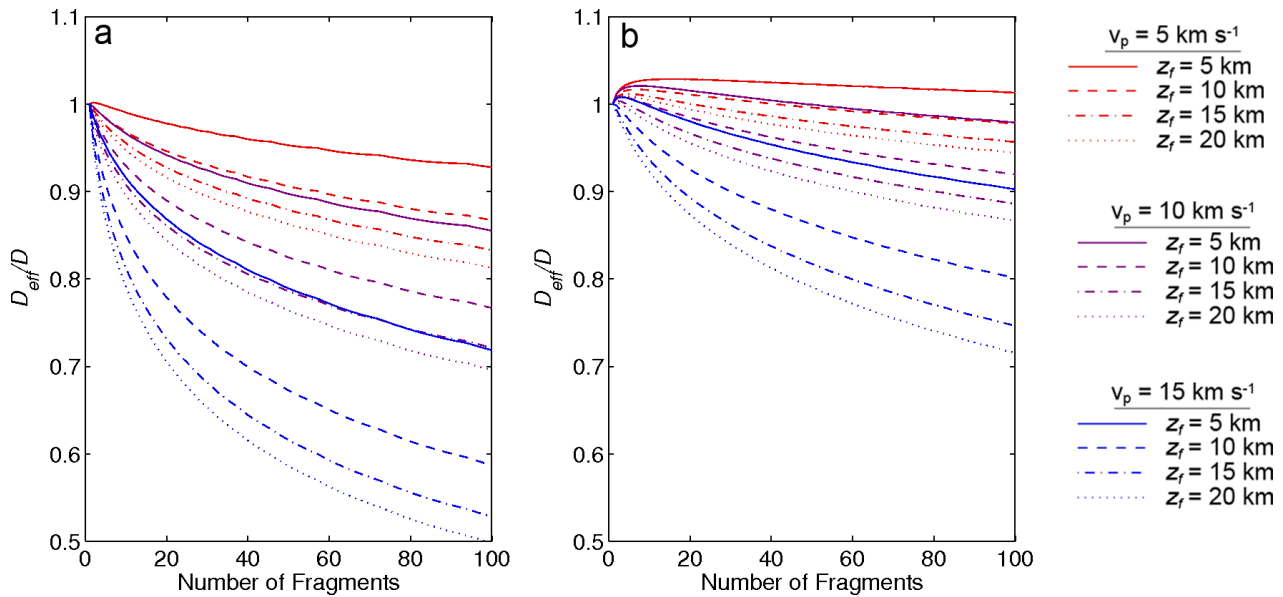


Figure 2: The ratio of D_{eff}/D versus N for initial projectile diameters (a) 50 cm, and (b) 1 m.

tion of the number of fragments, N , with the corresponding crater diameter, D , generated by an equivalent unfragmented impactor. Fig 2 shows the ratio D_{eff}/D for two impactors with initial $D_p = 50$ cm and 1 m, just prior to fragmentation with velocities $v_p = 5 - 15$ km s⁻¹ and fragmentation altitudes $z_f = 5 - 20$ km. All resulting craters are within the diameter range $\sim 1 - 6$ m. For simplicity, fragments are assumed to be equal divisions of the parent projectile, i.e. fragment masses equal m_p/N .

The ratio D_{eff}/D decreases with increasing N , velocity, and time of flight as smaller and faster individual fragments experience more drag and ablation resulting in greater deviation of D_{eff} from D with $D_{eff} \sim \frac{1}{2}D$ for the $D_p = 50$ cm object with $v_p = 15$ km s⁻¹ and $z_f = 20$ km representing the most extreme case. For the $D = 1$ m projectile, $D_{eff}/D > 1$ in some cases. This is a result of the dependence of impactor size on gravity-scaling. Crater efficiency decreases with increasing impactor size. In other words, the crater efficiency is larger for the fragments than for the parent projectile. As N increases, fragments shift increasingly into the strength-scaling regime and deceleration and ablation increase.

Summary: Initial results show the error introduced in estimates of D_{eff} are likely to be small for larger, slower projectiles, but D_{eff} begins to deviate significantly for the craters formed with smaller, higher velocity fragments, corresponding generally to craters with $D \lesssim 2$ m in our results. Our results also show the transition between strength-scaling

and gravity-scaling influences D_{eff}/D . We have shown results for regolith characterized by a single set of material properties, however variations in regolith properties will introduce additional uncertainty.

References

- [1] M. C. Malin, *et al.* Present impact cratering rate and the contemporary gully activity on Mars: Results of the mars global surveyor extended mission. *Science*, 314:1573–1557, 2006.
- [2] I. J. Daubar, *et al.* The current martian cratering rate. *Lunar Planet. Sci. Conf.*, XXXXI, 2010.
- [3] B. Ivanov, *et al.* Small impact crater clusters in high resolution HiRise images. *Lunar Planet. Sci. Conf.*, XXXIX, 2008.
- [4] B. Ivanov, *et al.* Small impact crater clusters in high resolution HiRise images - II. *Lunar Planet. Sci. Conf.*, XXXX, 2009.
- [5] B. Ivanov, *et al.* New small impact crater in high resolution HiRise images - III. *Lunar Planet. Sci. Conf.*, XXXXI, 2010.
- [6] Z. Ceplecha, *et al.* Meteor phenomena and bodies. *Space Sci. Rev.*, 84:327–471, 1998.
- [7] J.-P. Williams, *et al.* The production of small primary craters on Mars. *Lunar Planet. Sci. Conf.*, XXXXI, 2010.
- [8] P. Davis. Meteoroid impacts as seismic sources on Mars. *Icarus*, 105:469–478, 1993.
- [9] O. Popova, *et al.* Very low strengths of interplanetary meteoroids and small asteroids. *Meteoritics and Planetary Science*, 47:1525–1550, 2011.
- [10] K. A. Holsapple. The scaling of impact processes in planetary science. *Ann. Rev. Earth Planet. Sci.*, 21:333–373, 1993.